Towards 100,000-pixel microcalorimeter arrays using multi-absorber transition-edge sensors

Presented by Stephen Smith NASA Goddard Space Flight Center

Key contributors:
NASA GSFC: J.S. Adams, S.R. Bandler, S. Beaumont, J.A. Chervenak, A.M. Datesman, M.E. Eckart (LLNL), F.M. Finkbeiner, R. Hummatov, R.L. Kelley, C.A. Kilbourne, A.R. Miniussi, F.S. Porter, J.S. Sadleir, K. Sakai, N. Wakeham, E.J. Wassell, M.C. Witthoeft.
Lincoln Labs MIT: K. Ryu.

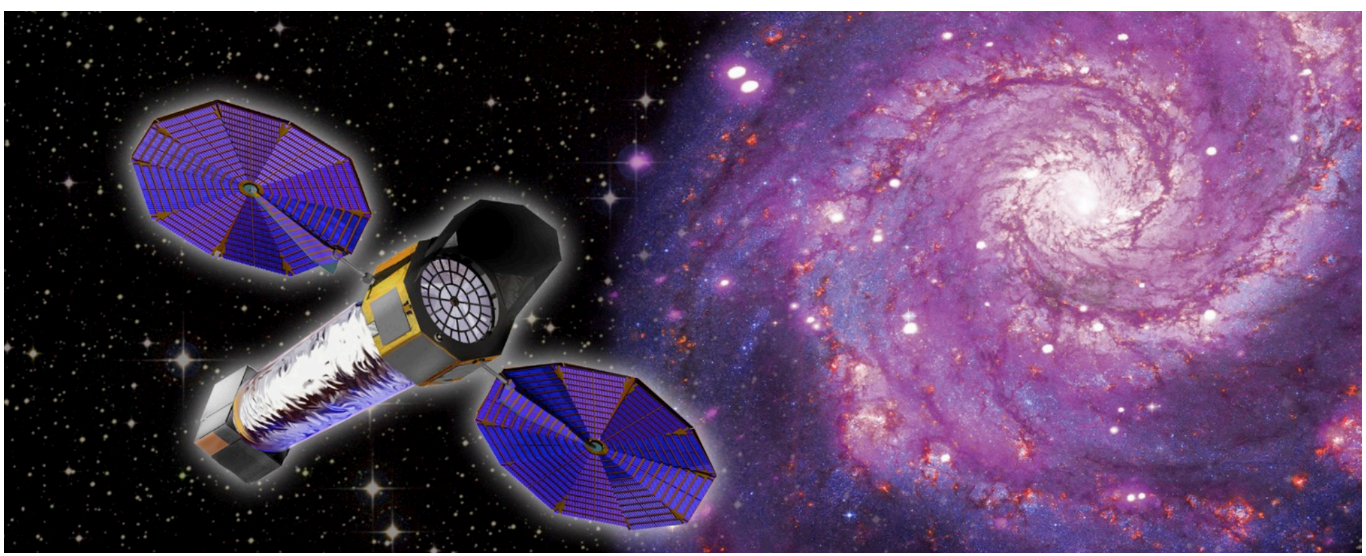

Microcalorimeters for imaging and high resolution spectroscopy

- Microcalorimeters are ideal detectors for next gen. X-ray space telescopes.

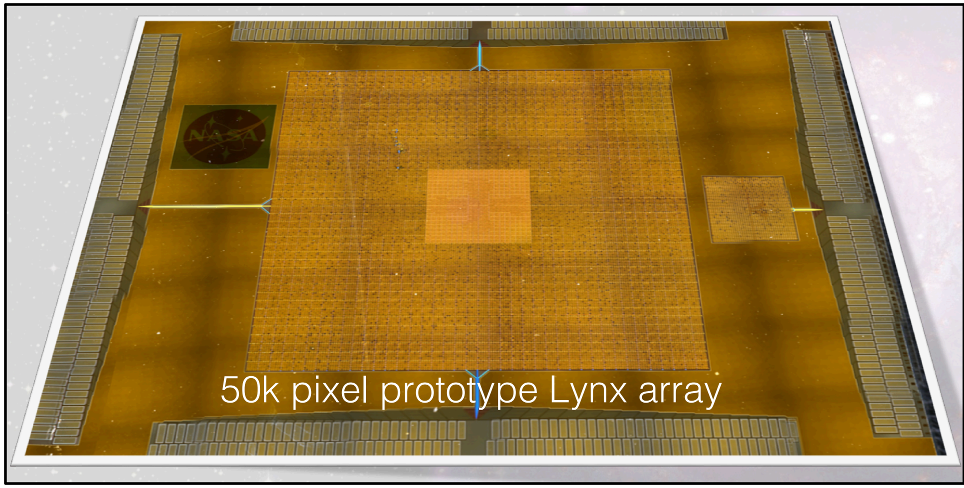

- NASA's Lynx X-ray Telescope
  - Proposed launch late 2030's.
  - 5′ field-of-view + 0.5-1.0″ angular resolution.

  => 100,000 pixels, 25-50 μm pitch.
  - ΔE_{FWHM} < 3 eV @ 7 keV.

- Lynx requirements extremely challenging.
  - Not practical if 1 pixel = 1 TES.
  - Prohibitively high density of wiring on detector chip.
  - Space needed for large # of bias circuit and readout components (shunt resistors, inductors, u-mux resonators etc).

- Practical solution: Exploring the use of multi-absorber TESs + 3d buried wiring layers.

Sub-μm multi-layer wiring

- Buried wiring layers.
  - Collaborating with MIT / Lincoln Laboratory.
  - High yield, planarized, multi-layer (0.5 μm width) Nb wiring.
  - TES fabricated at NASA GSFC on top of polished SiO_2 surface.
  - Enables high density of wiring within array.

See poster **11-94. J. Chervenak et al.**
And later talk **221. T. Stevenson et al.**
for fabrication details on this

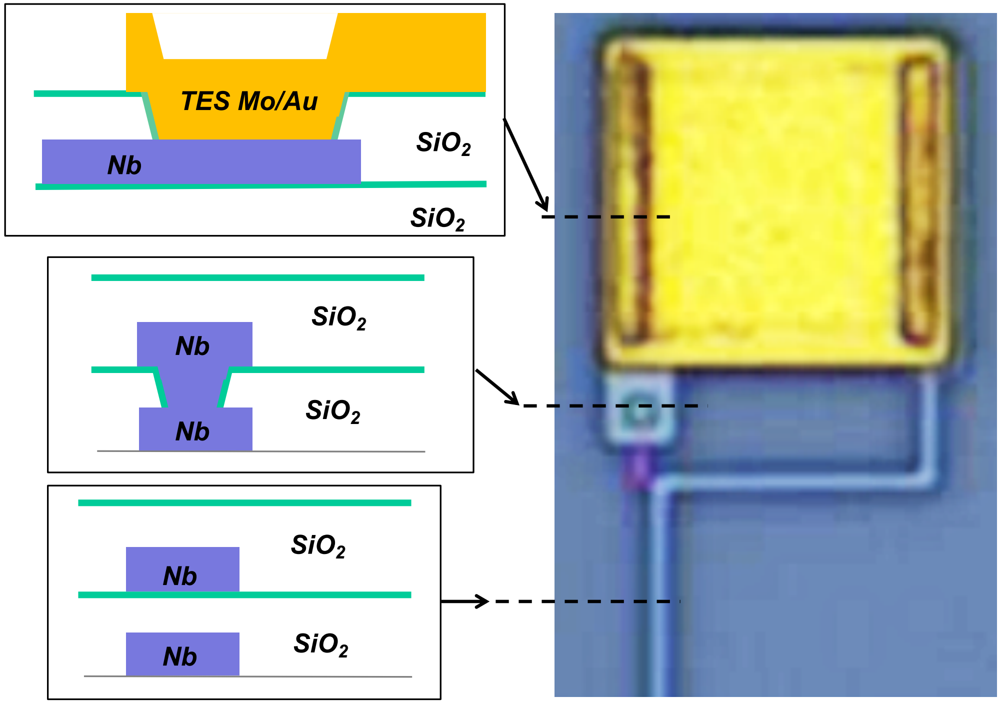

Multi-absorber TES 'Hydras'.

- Multiple absorbers with a different thermal conductance to a single readout sensor.
  - Different characteristic pulse shape for each element within the hydra.
  - Enables position discrimination between pixels.
- Introduction of position discrimination comes at some trade with ΔE

(1) Internal thermal fluctuation noise between absorbers and TES.

(2) Reduced signal bandwidth relative to the noise.

ΔE_{FWHM} typically 1.2 -1.3 x worse than single pixel with same total heat capacity

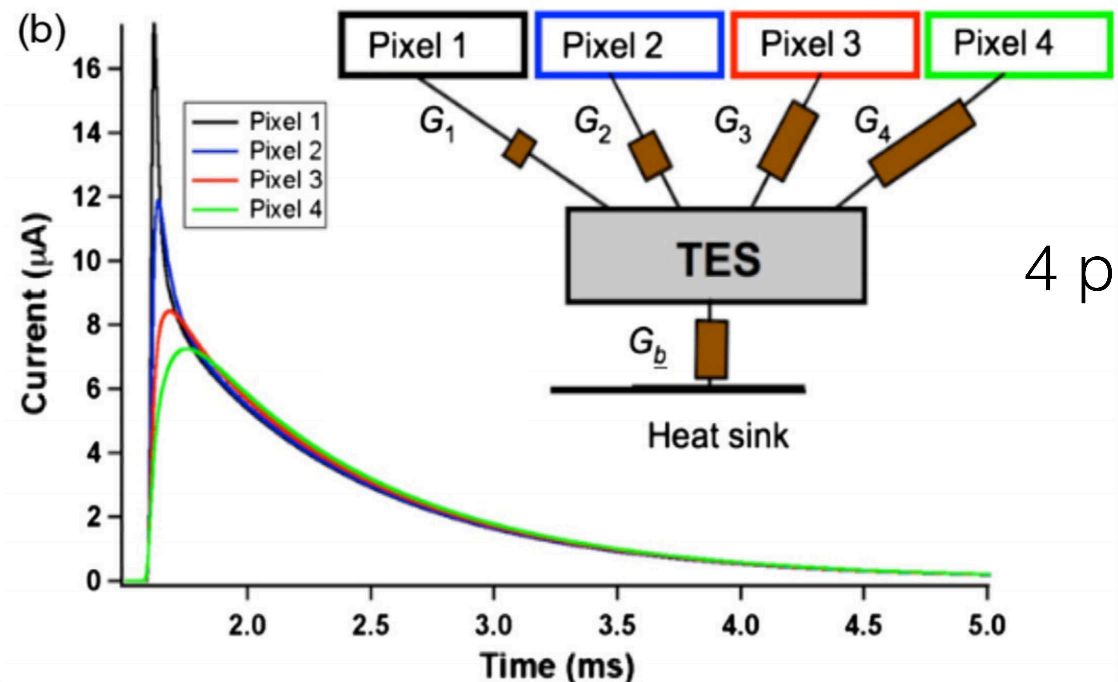

4 pixel hydra

Lynx X-ray Microcalorimeter (LXM) Array Concept

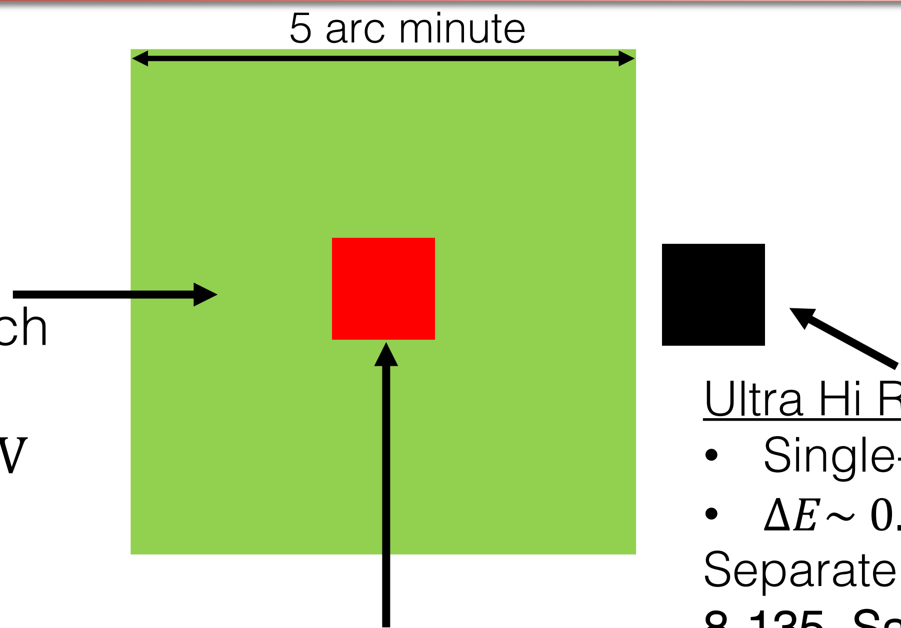

Main Array
- 25-pixel hydras
- 1”, 50 μm pixel pitch
- 86k pixels
- $\Delta E \sim 3\ \mathrm{eV}, E < 7\ \mathrm{keV}$

Ultra Hi Res Array
- Single-pixel array
- $\Delta E \sim 0.3\ \mathrm{eV}, E < 0.7\ \mathrm{keV}$

Separate poster on this:
8-135. Sakai et al.

Enhanced Main Array
- 25-pixel hydras
- 0.5”, 25 μm pixel pitch
- 13k pixels
- $\Delta E \sim 2\ \mathrm{eV}, E < 7\ \mathrm{keV}$

100,000 pixels with only 4000 TESs
read out with microwave mux

25-pixel hydras for Lynx

- Previous hydras all links connect to TES.
- Example here shows 'tree' geometry
  - Hierarchical link structure ('trunk' and 'branches')
  - Not all absorbers connect directly to the TES.
  - Easier to layout with large # of absorbers.
  - More complicated pre-equilibration signal.

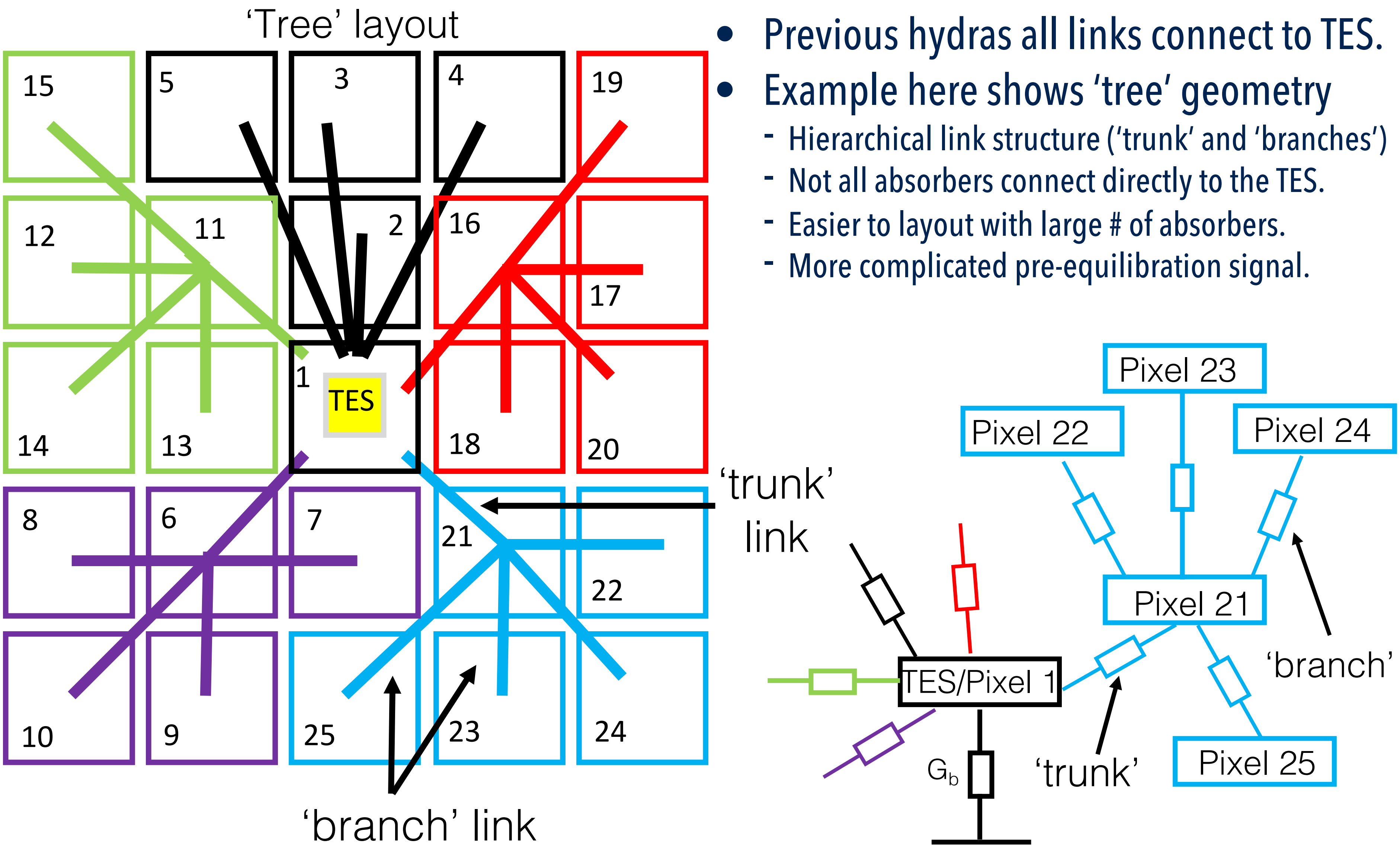

25-pixel hydras for Lynx

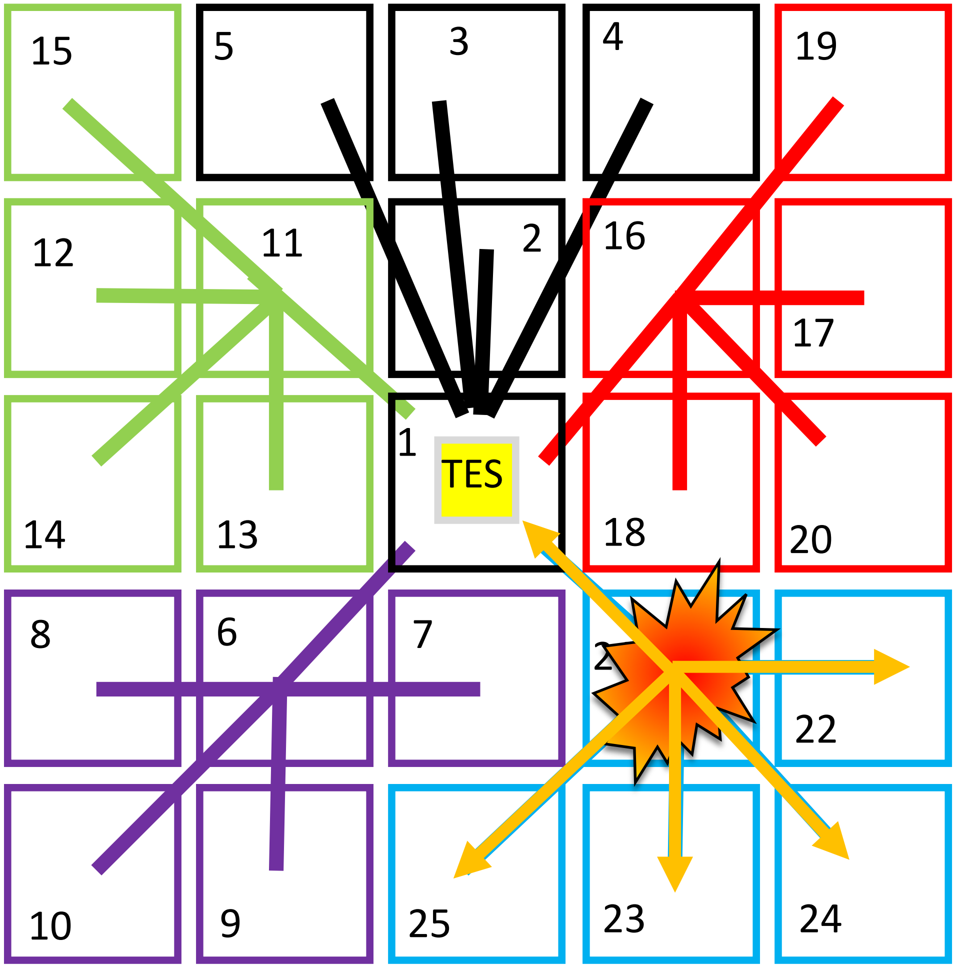

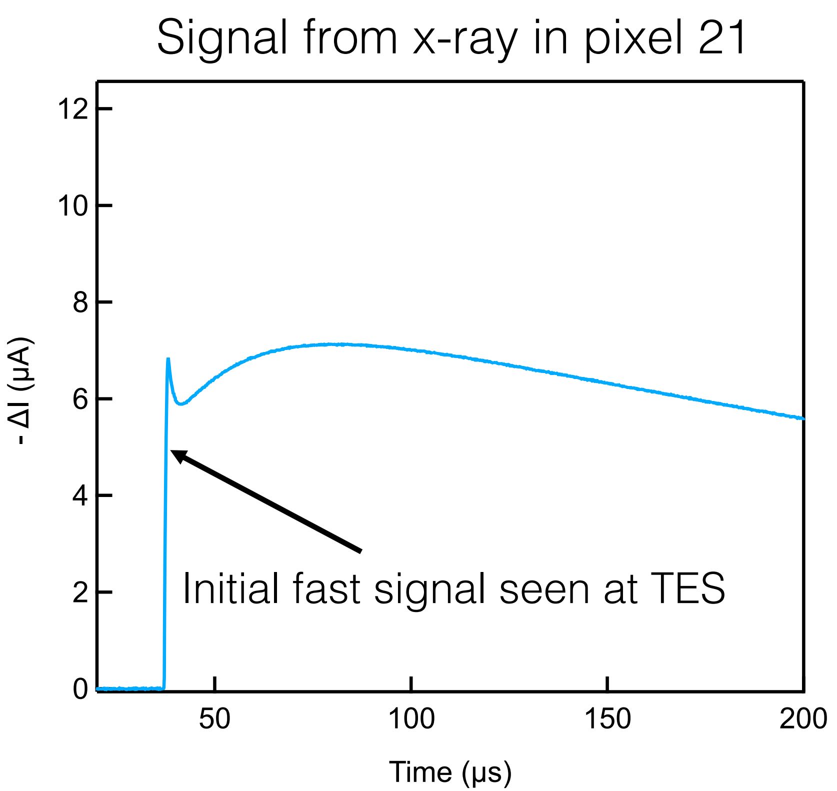

25-pixel hydras for Lynx

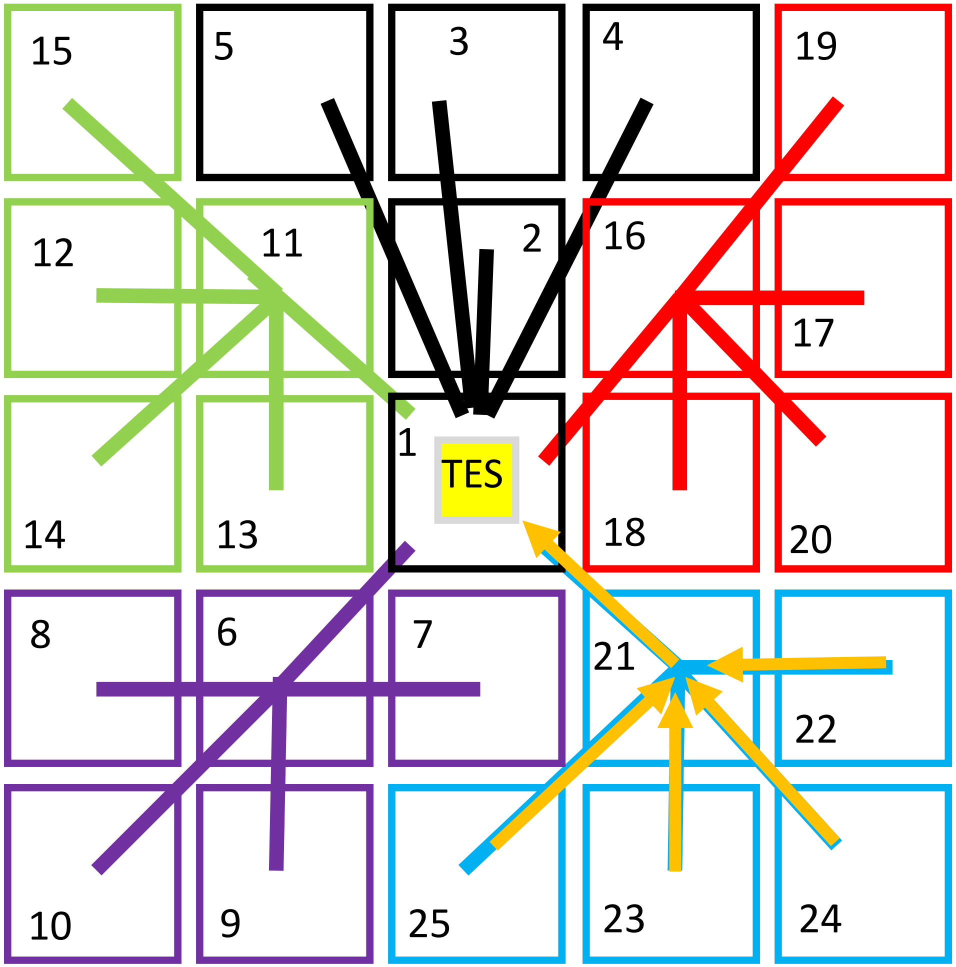

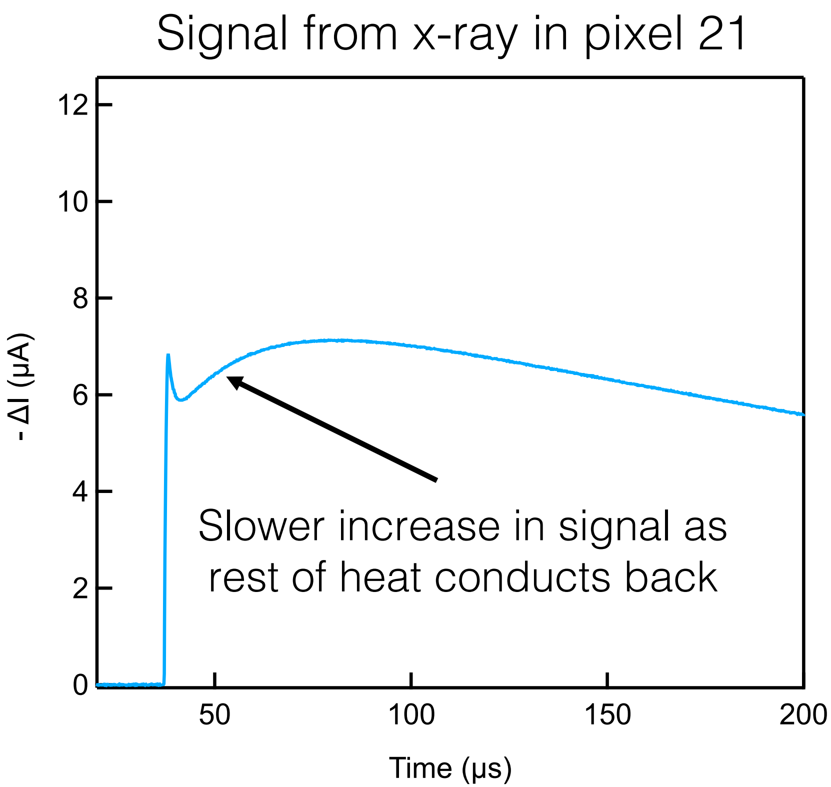

25-pixel hydras for Lynx

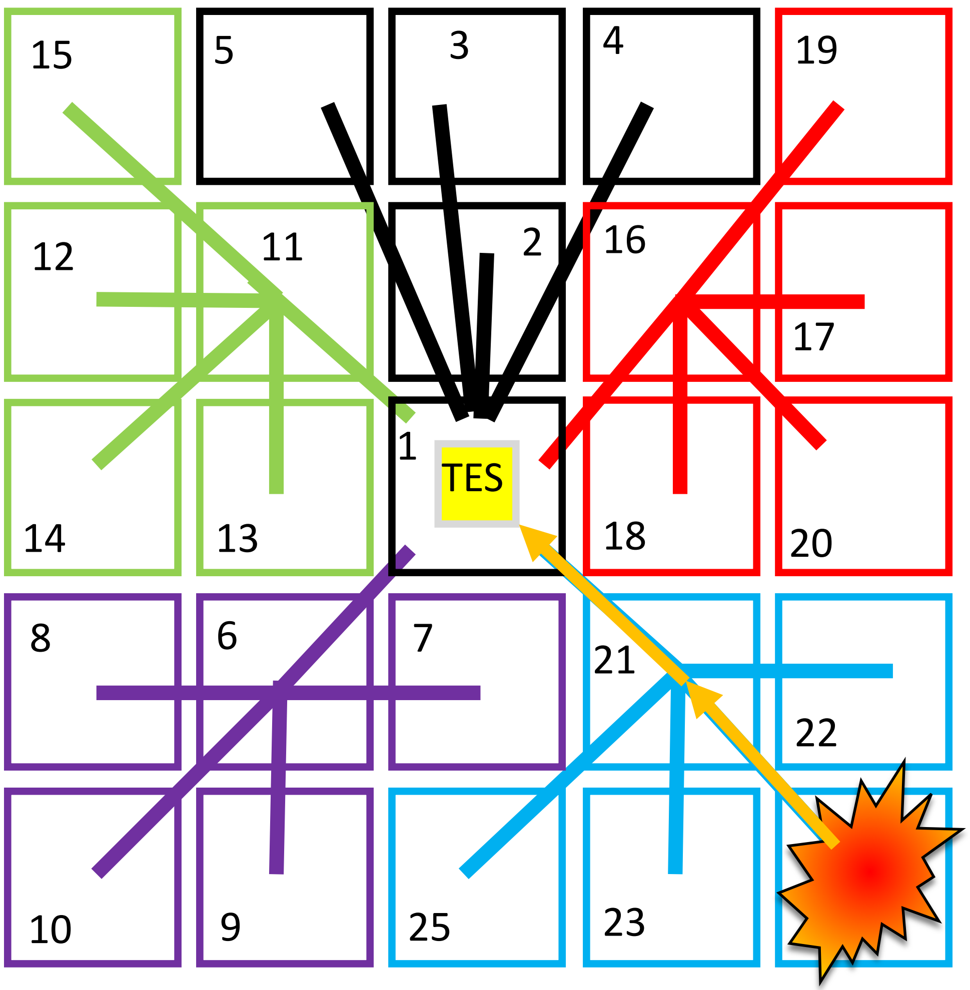

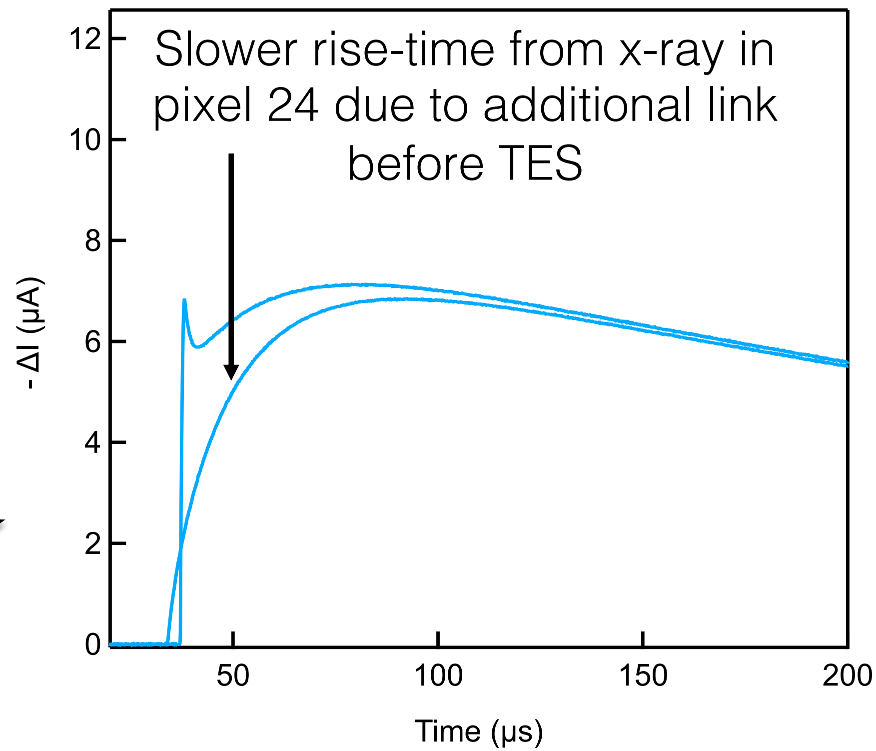

25-pixel hydras for Lynx

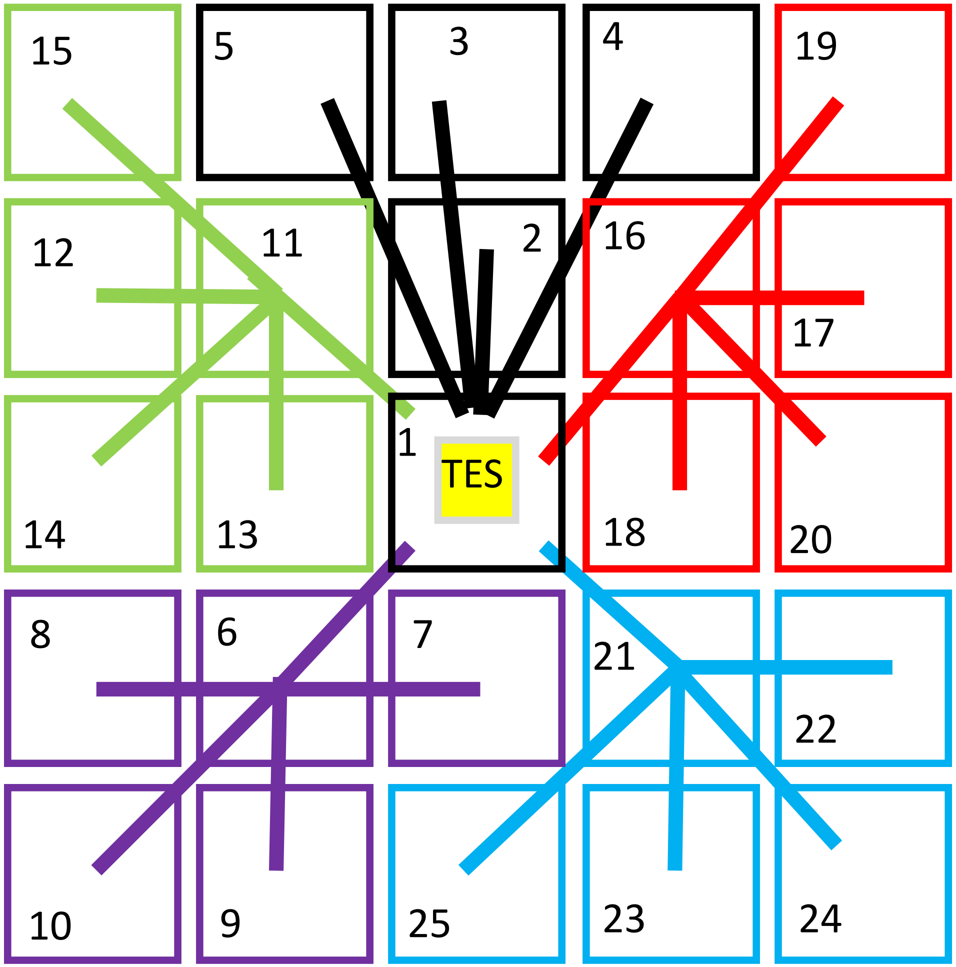

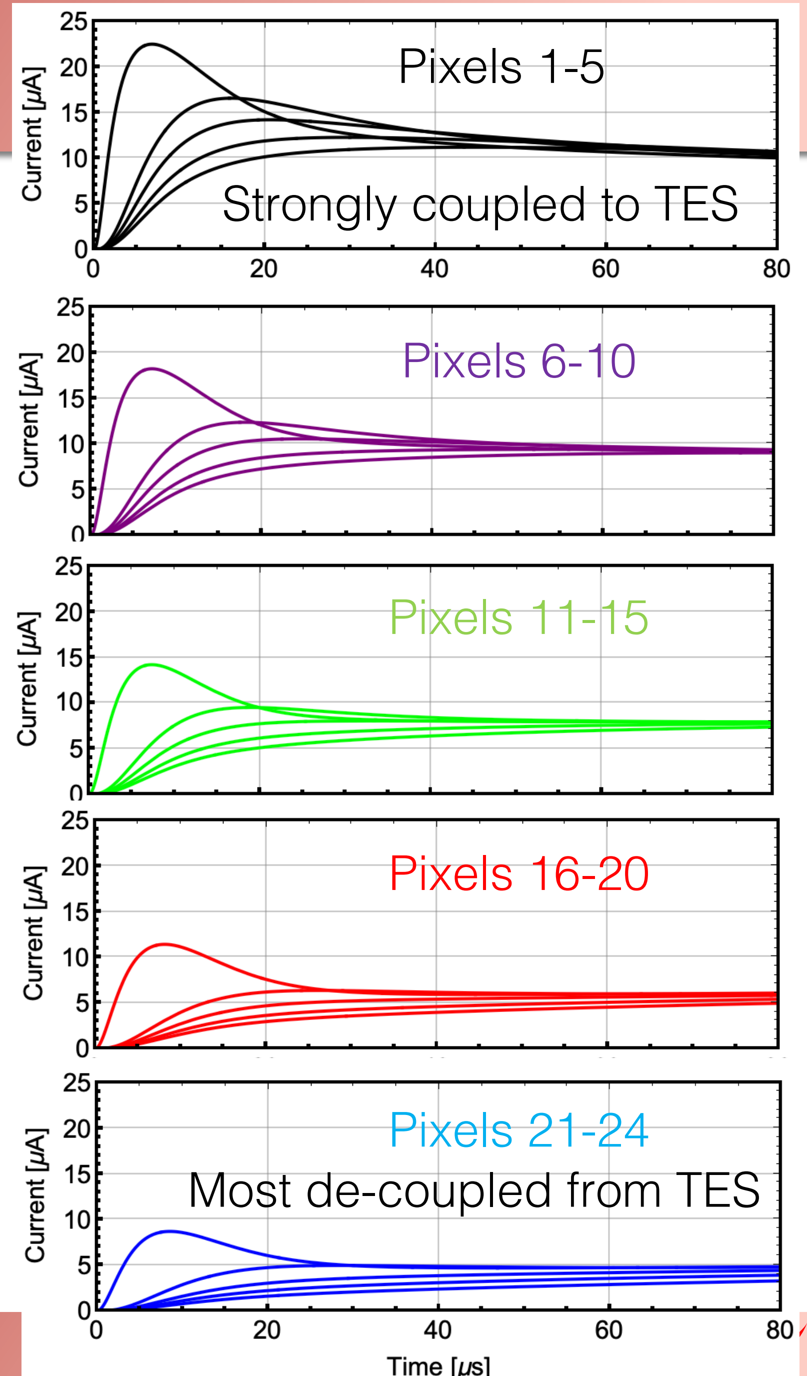

Fabricated first prototype Lynx arrays with 25-absorbers / TES.

- Example here shows 50,000 pixel array (half final requirement).
- Includes:
  - 25-pixel hydras with 25 μm and 50 μm absorber pitch.
  - Includes 3d buried wiring.
- No back-side Au heat-sink layers yet. (susceptible to thermal noise from x-talk)

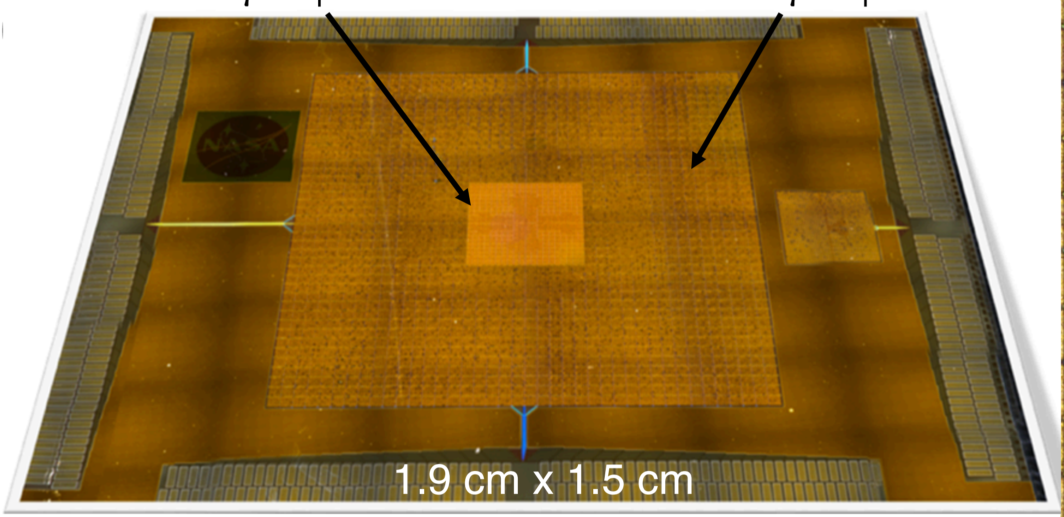

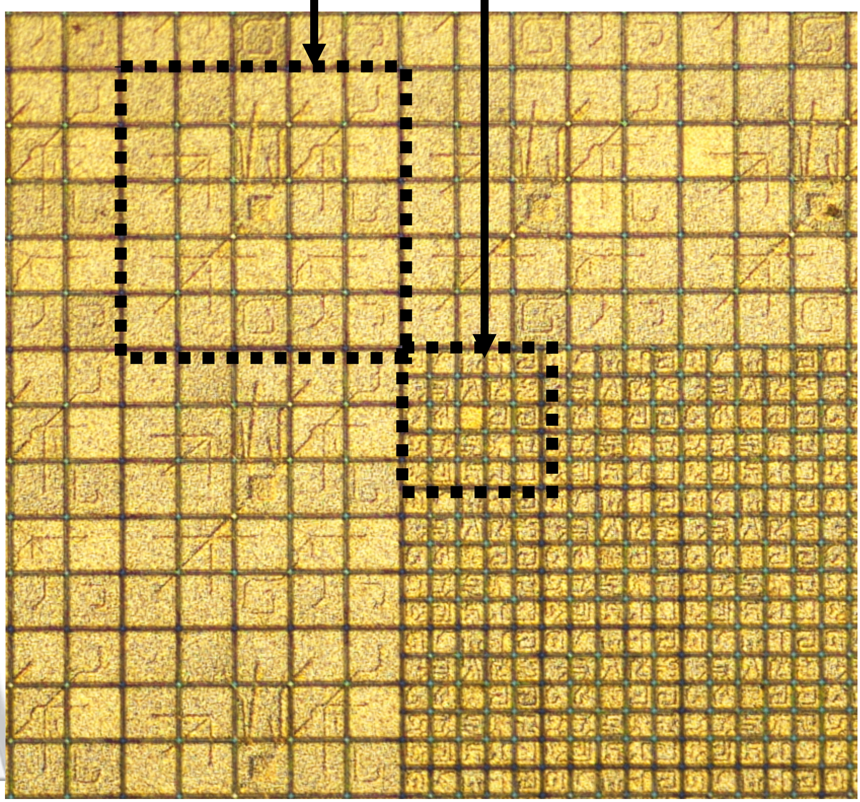

25-pixel hydra layout - 25 μm pitch absorbers

- 20 μm Mo/Au TES, $T_0 = 50$ mK
- Total C = 0.1 pJ/K
- Au links 1-2 μm widths,
  300 nm thick
- Vary length of link to tune *G*.
- 25x Au absorbers, 25 μm pitch, 3.2 μm thick.
- Absorbers cantilevered above the substrate, contact links at single point.

Hydra before absorber deposition

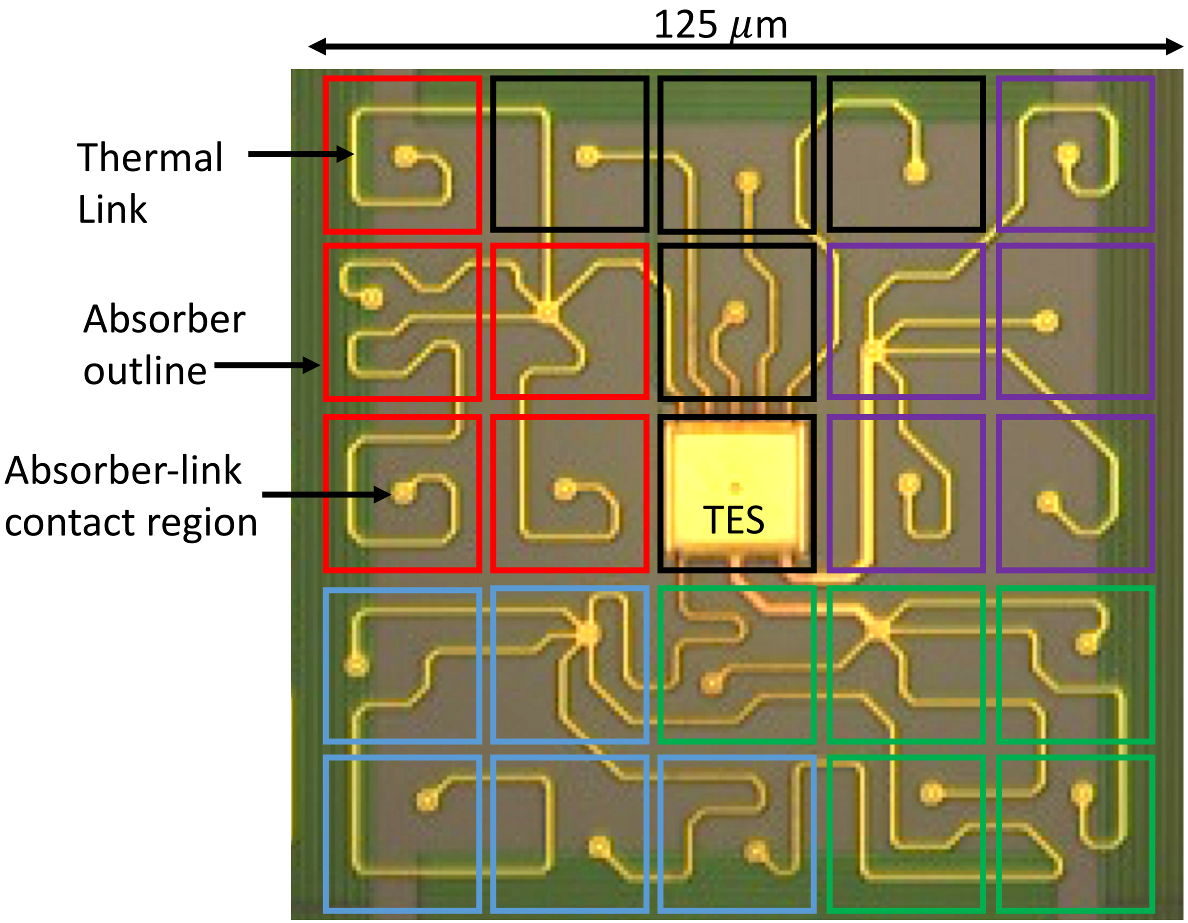

25-pixel hydra measured pulse shapes at 1.5 keV (Al-Kα x-rays)

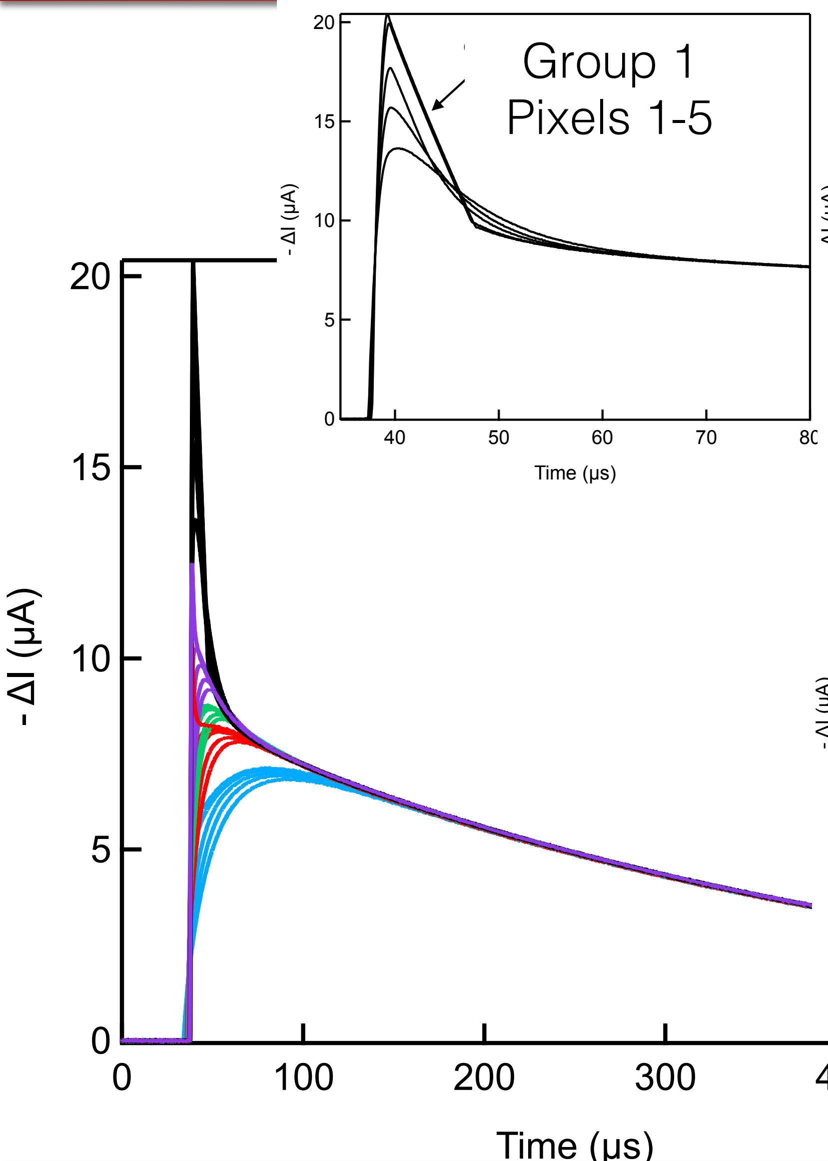

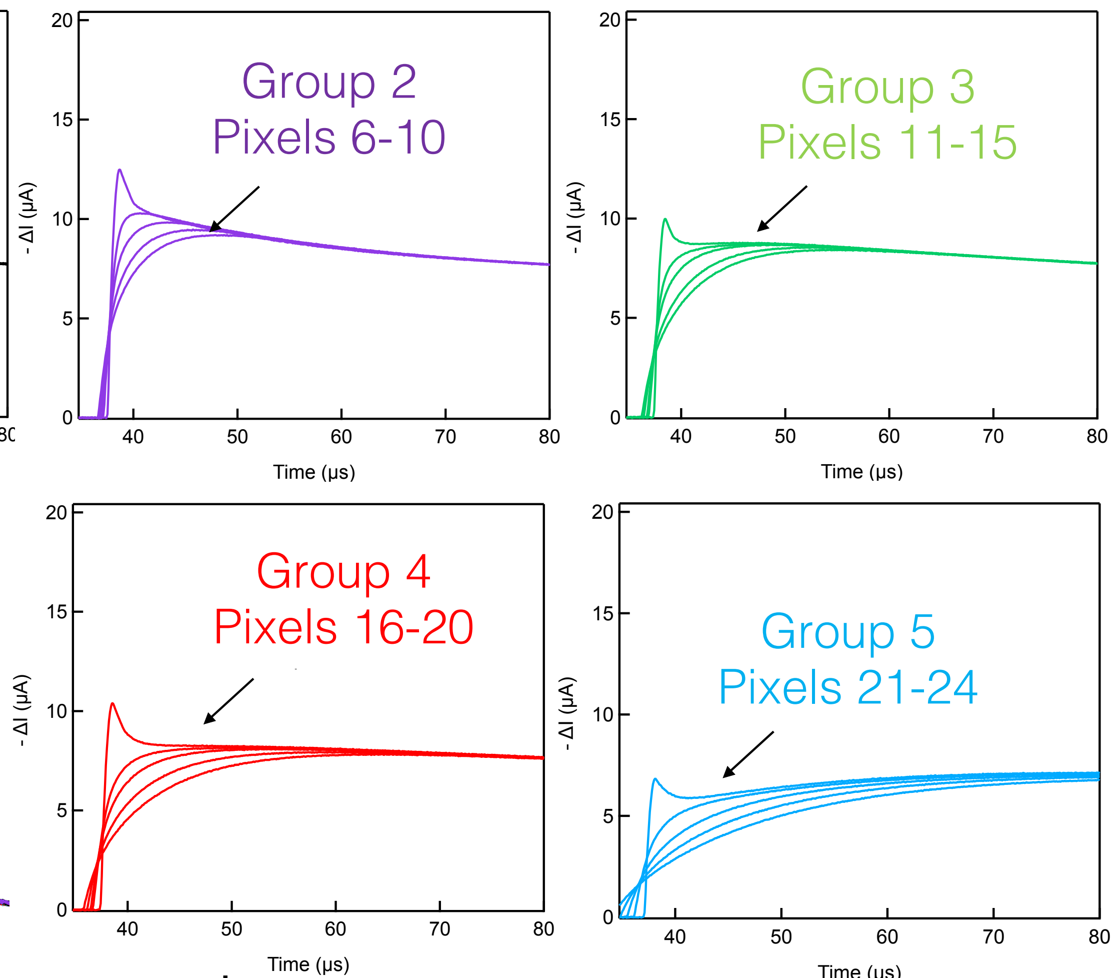

- 1st results obtained in the last few weeks.

25-pixel hydra position discrimination

- Variety of different potential metrics to characterize pulse shape.
- Different discrimination algorithms studied in detail in **Poster 153. Beaumont et al.**
- Example here is simple but reasonably effective on all pixels.
  - Uses 2 parameterizations of the rise-time.
  - X-axis slow rise-time from smoothed pulse
  - Y-axis fast rise-time from unsmoothed pulse

rise-time scatter plot for 25 pixel hydra
Al-Kα x-rays (1.5 keV)

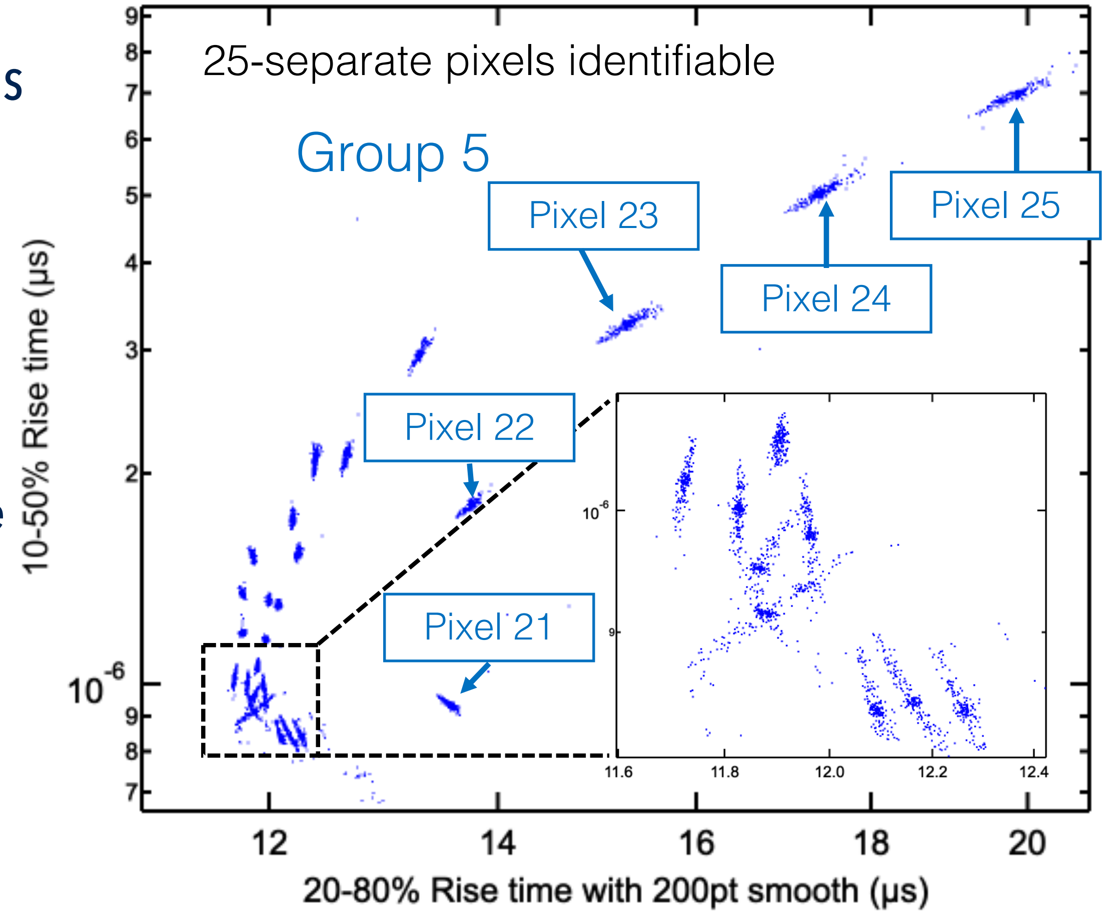

25-pixel hydra position discrimination

- Variety of different potential metrics to characterize pulse shape.
- Different discrimination algorithms studied in detail in **Poster 153. Beaumont et al.**
- Example here is simple but reasonably effective on all pixels.
  - Uses 2 parameterizations of the rise-time.
  - X-axis slow rise-time from smoothed pulse
  - Y-axis fast rise-time from unsmoothed pulse

rise-time scatter plot for 25 pixel hydra
Al-Kα x-rays (1.5 keV)

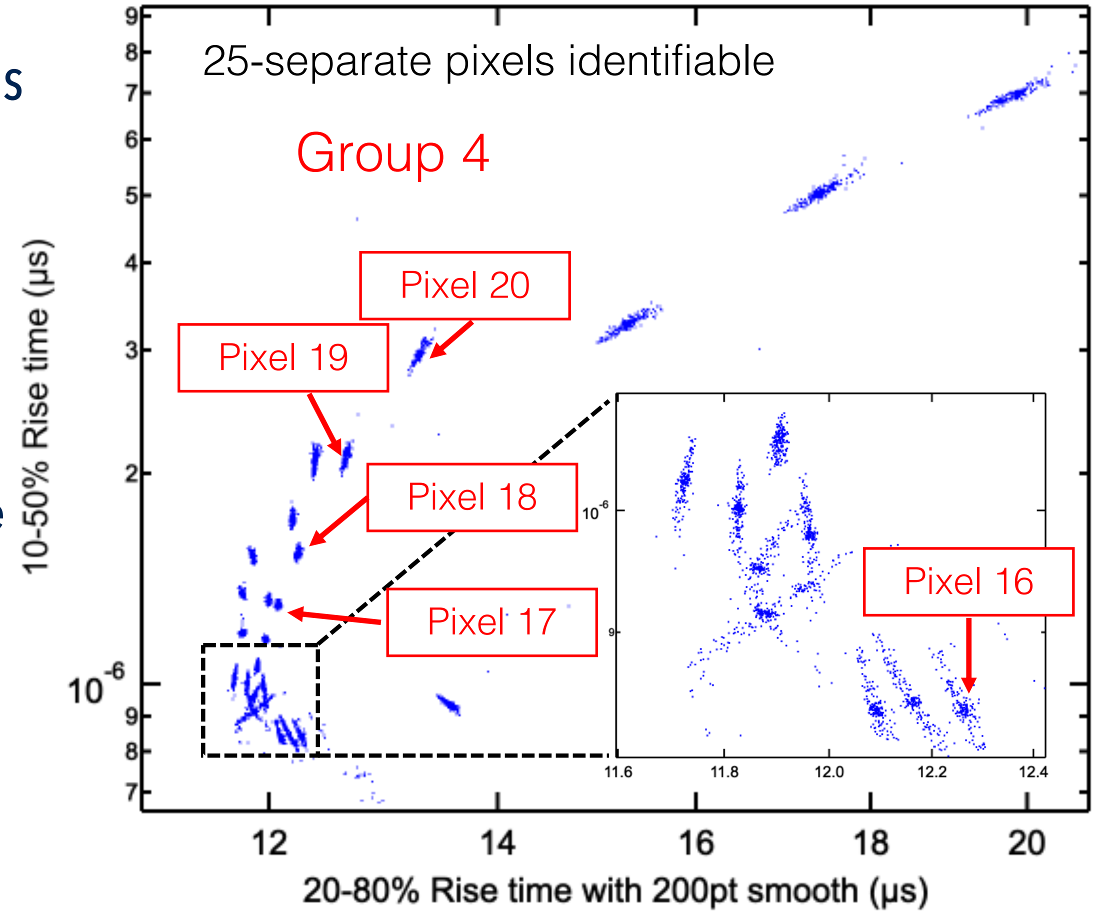

25-pixel hydra position discrimination

- Variety of different potential metrics to characterize pulse shape.
- Different discrimination algorithms studied in detail in **Poster 153. Beaumont et al.**
- Example here is simple but reasonably effective on all pixels.
  - Uses 2 parameterizations of the rise-time.
  - X-axis slow rise-time from smoothed pulse
  - Y-axis fast rise-time from unsmoothed pulse

rise-time scatter plot for 25 pixel hydra Al-Kα x-rays (1.5 keV)

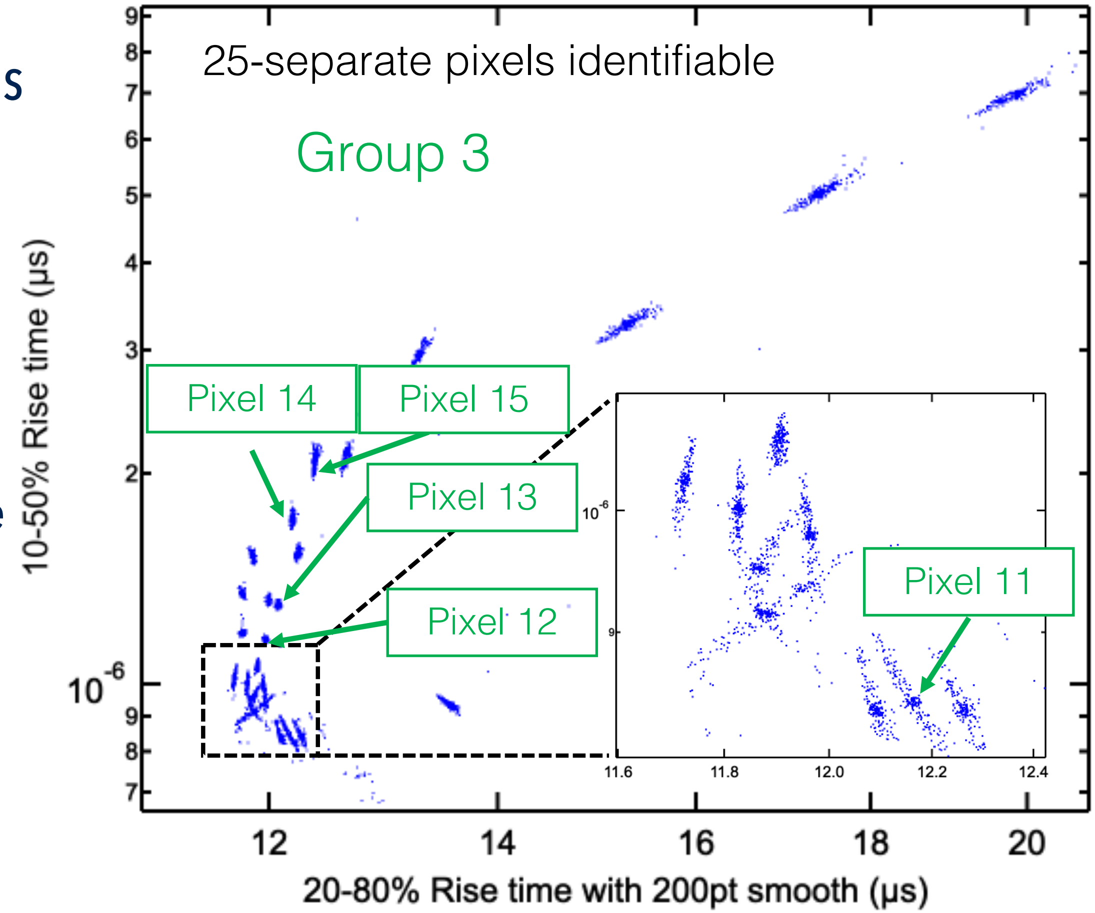

25-pixel hydra position discrimination

- Variety of different potential metrics to characterize pulse shape.
- Different discrimination algorithms studied in detail in **Poster 153. Beaumont et al.**
- Example here is simple but reasonably effective on all pixels.
  - Uses 2 parameterizations of the rise-time.
  - X-axis slow rise-time from smoothed pulse
  - Y-axis fast rise-time from unsmoothed pulse

rise-time scatter plot for 25 pixel hydra Al-Kα x-rays (1.5 keV)

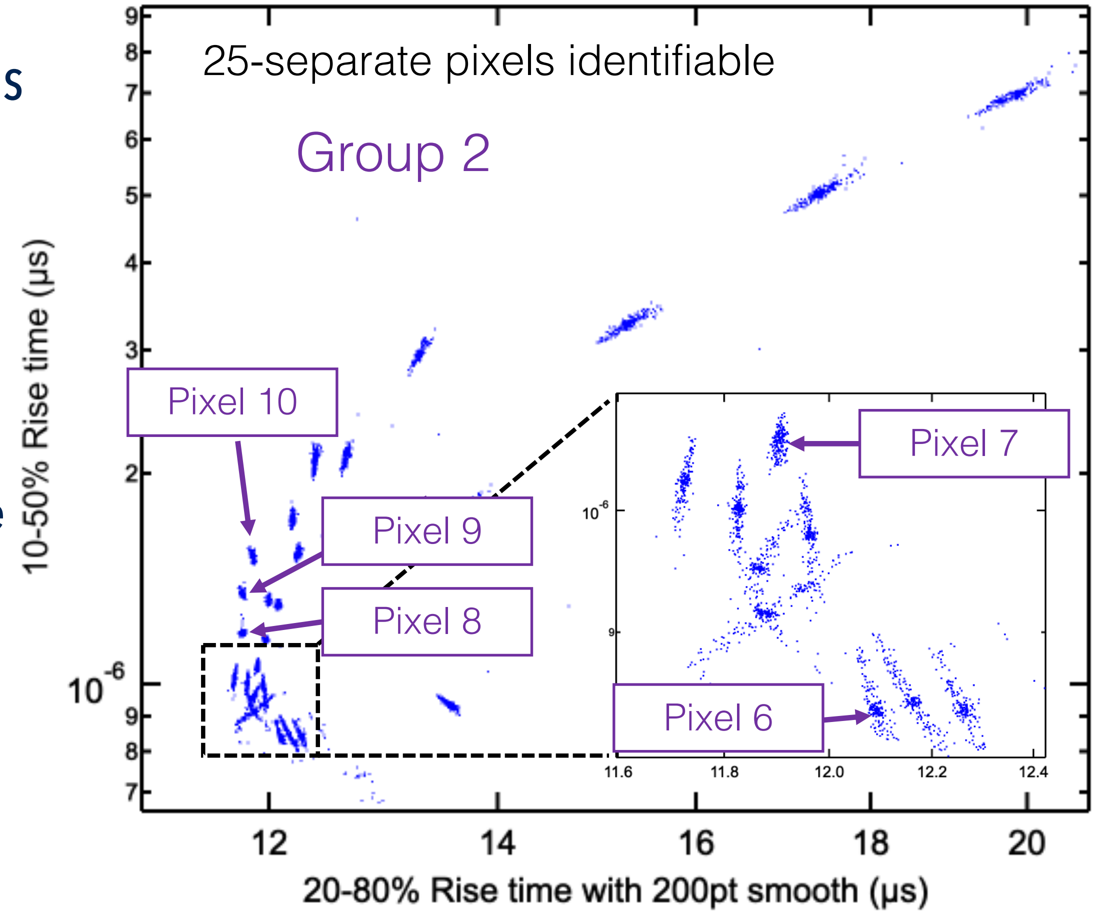

25-pixel hydra position discrimination

- Variety of different potential metrics to characterize pulse shape.
- Different discrimination algorithms studied in detail in **Poster 153. Beaumont et al.**
- Example here is simple but reasonably effective on all pixels.
  - Uses 2 parameterizations of the rise-time.
  - X-axis slow rise-time from smoothed pulse
  - Y-axis fast rise-time from unsmoothed pulse

rise-time scatter plot for 25 pixel hydra
Al-Kα x-rays (1.5 keV)

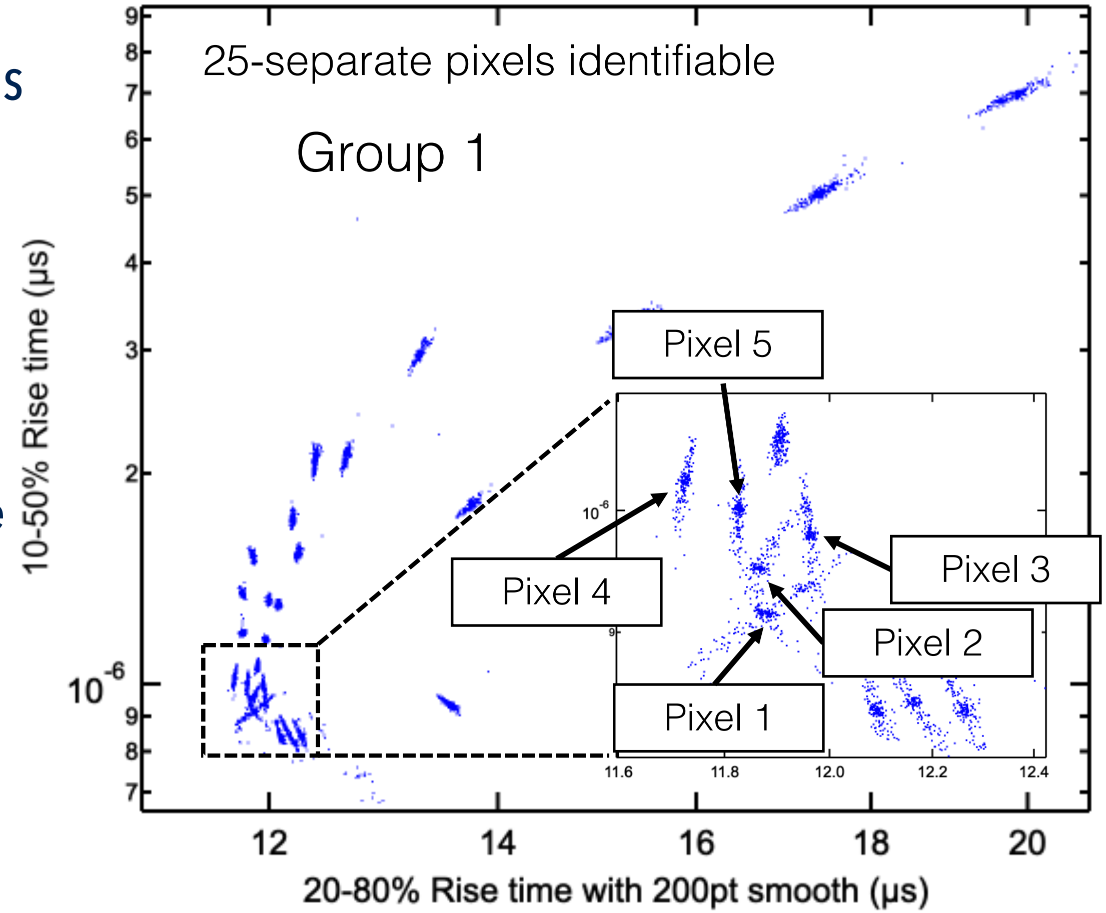

25-pixel hydra position discrimination

- Energy dependence still needs to be explore (0.2-7 keV).
  - Broader distributions at low E (worse signal to noise).
  - Possibly broader at higher E because of non-linear.

rise-time scatter plot for 25 pixel hydra Al-Kα x-rays (1.5 keV)

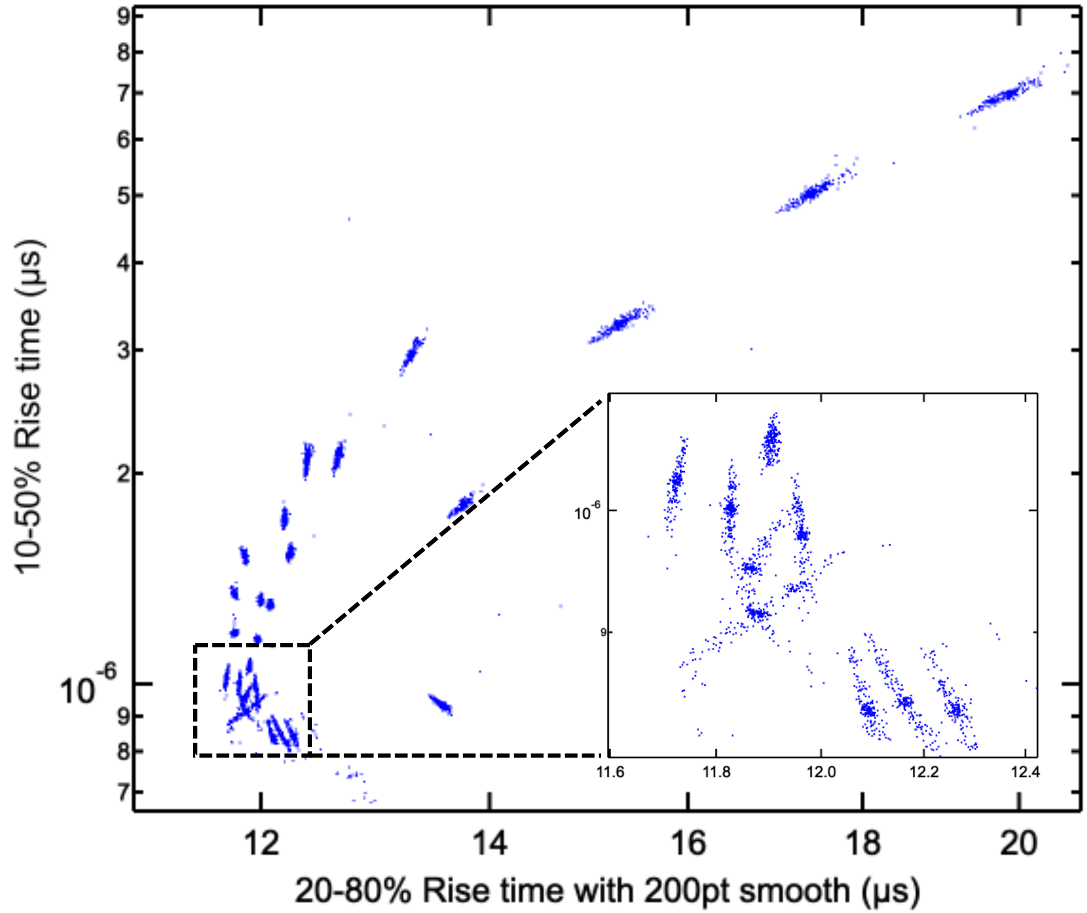

25-pixel hydra ΔE_{FWHM} - 25 μm pitch absorbers

- Measured $\Delta E_{FWHM} = 1.66 \pm 0.02eV$ (all pixels coadded).
- All pixels < 2eV, $\langle \Delta E_{FWHM} \rangle = 1.68 \pm 0.13eV$.
- Estimate effect of additional x-talk noise as 0.2 eV => ~1.5 eV possible (with heat-sinking).

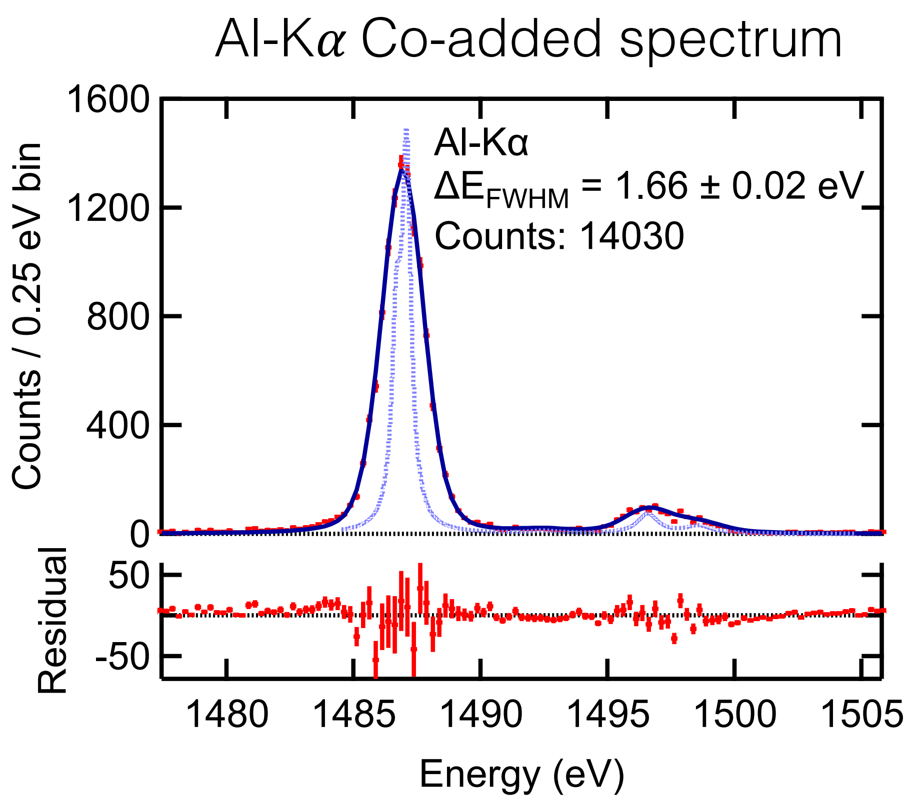

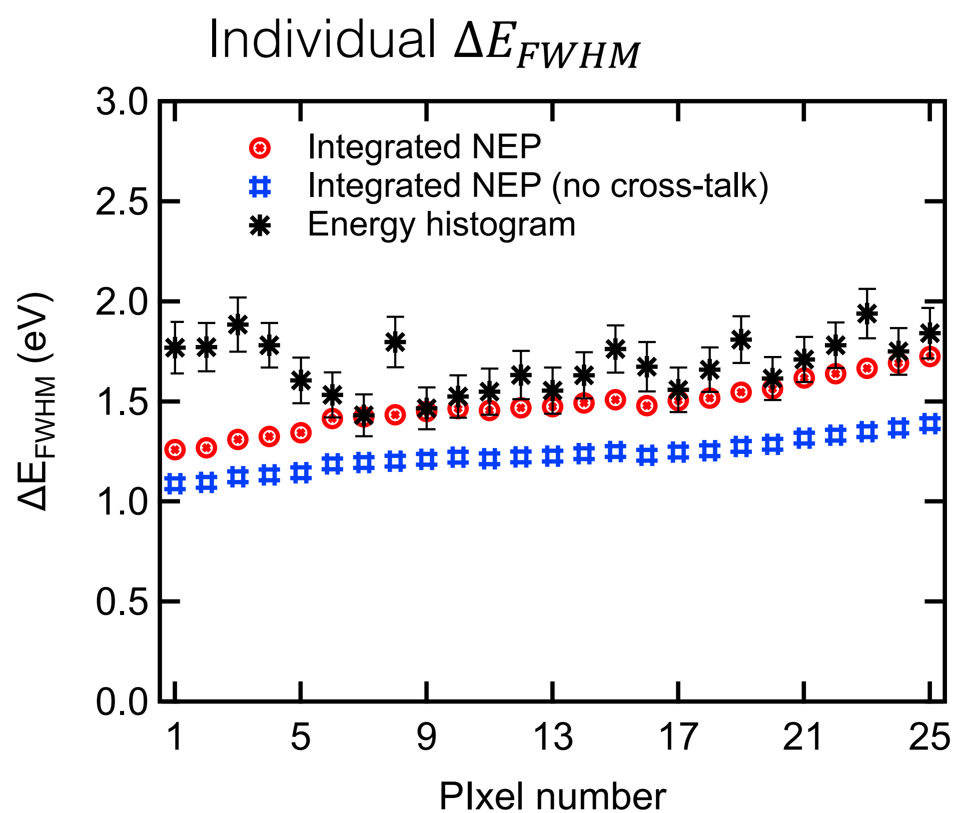

25-pixel hydra ΔE_{FWHM} - 50 μm pitch absorbers

- $\Delta E_{FWHM} \propto \sqrt{C}$ => ~2x worse than 25 μm pixel design.
- Measured $\Delta E_{FWHM} = 3.34 \pm 0.02 eV$ (all pixels coadded).
- Estimate effect of additional thermal noise as 0.4 eV => ~3 eV possible.
- 25-pixels identifiable.

Co-added Al-Kα spectrum

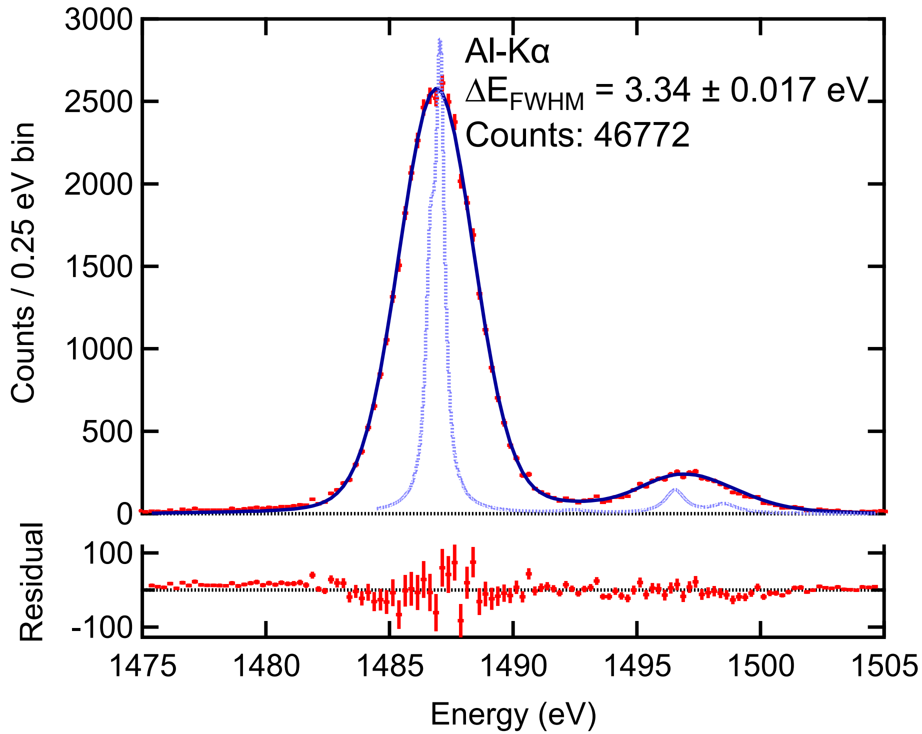

Average measured pulses

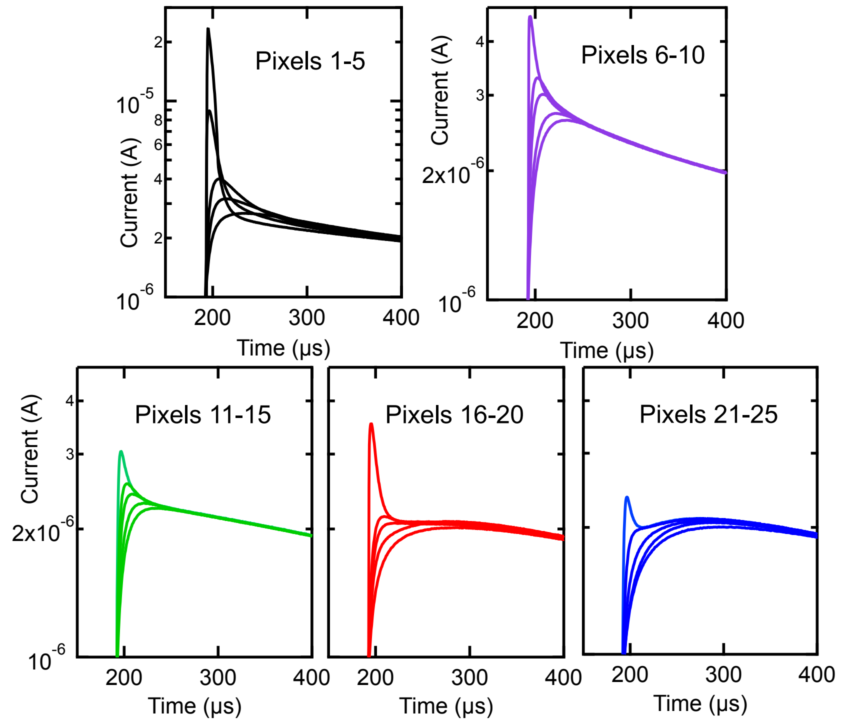

Summary and outlook

- Demonstrated 1st proof-of-concept results from 25-pixel hydras with buried wiring.
  - Achieved $\Delta E_{FWHM} = 1.66 \pm 0.02eV$ for $25\mu m$ version.
  - Achieved $\Delta E_{FWHM} = 3.34 \pm 0.02eV$ for $50\mu m$ version.
- Position discrimination was straightforward at 1.5 keV.
- Demonstrates feasibility of 100,000 pixel array for Lynx.

- Still to do:
  - Measure broad-band response up to 7 keV (resolution and position discrimination).
  - Next generation design will include back heatsinking layer for x-talk mitigation.
  - Study compatibility with state-of-the art readout systems (microwave mux).
    - Testing with higher inductance to slow-rise time and reduce slew-rate to match readout.

- ADDITIONAL BACK-UP MATERIAL

Effect of increasing inductance to slow rise-time

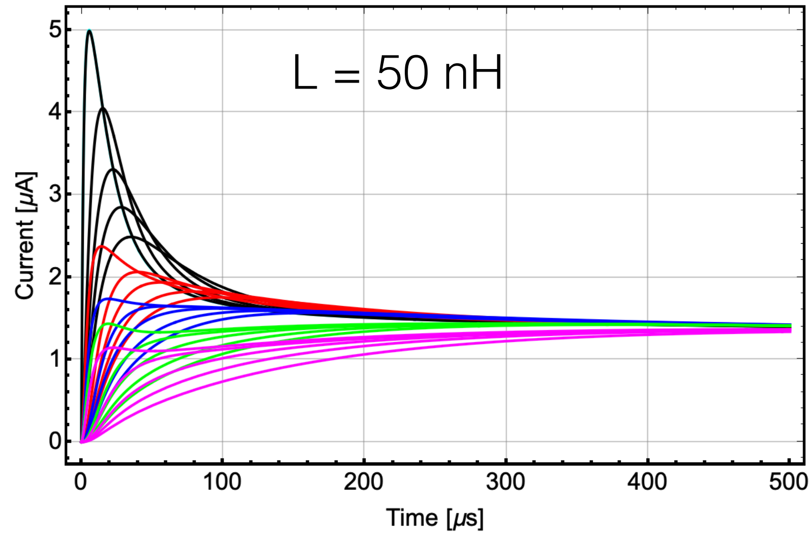

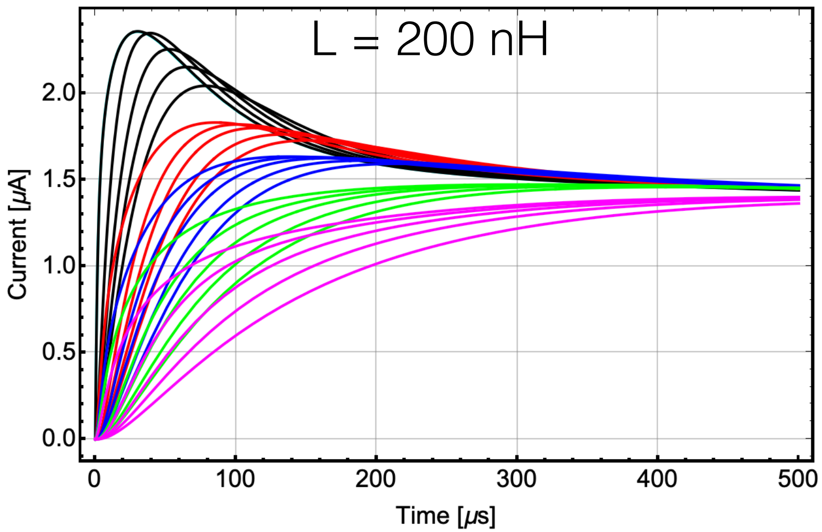

SEM Images

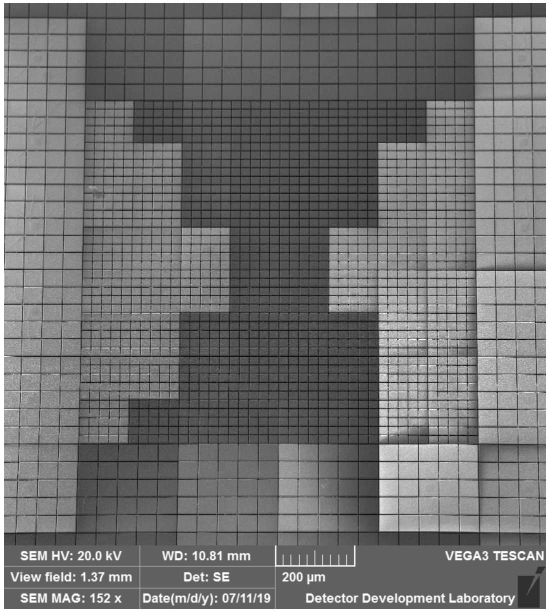
SEM HV: 20.0 kV
WD: 10.81 mm
VEGA3 TESCAN
View field: 1.37 mm
Det: SE
200 μm
SEM MAG: 152 x
Date(m/d/y): 07/11/19
Detector Development Laboratory

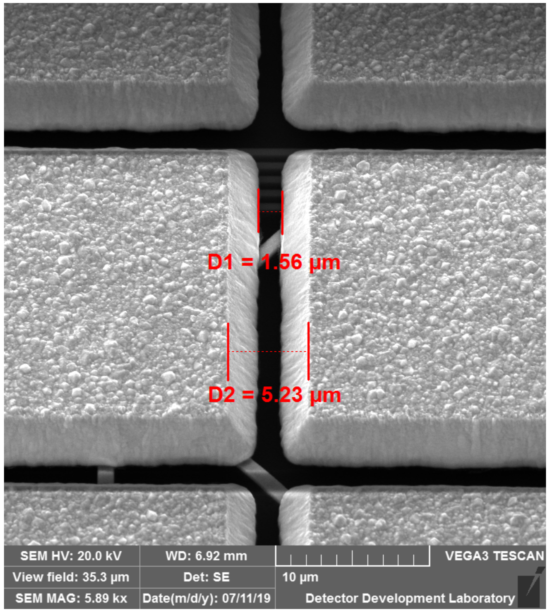
D1 = 1.56 μm
D2 = 5.23 μm
SEM HV: 20.0 kV
WD: 6.92 mm
VEGA3 TESCAN
View field: 35.3 μm
Det: SE
10 μm
SEM MAG: 5.89 kx
Date(m/d/y): 07/11/19
Detector Development Laboratory

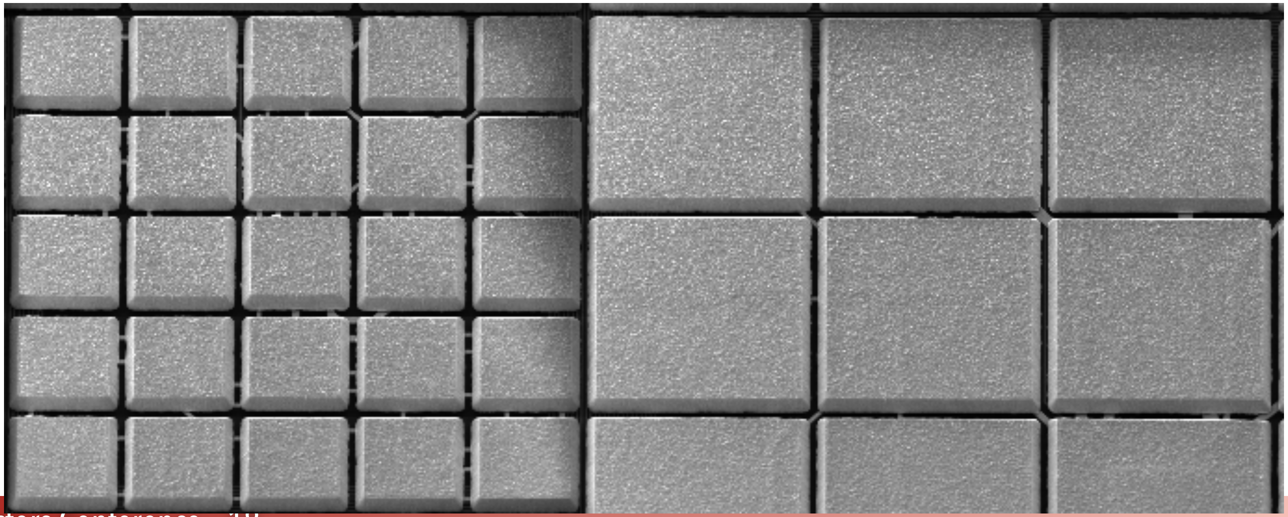

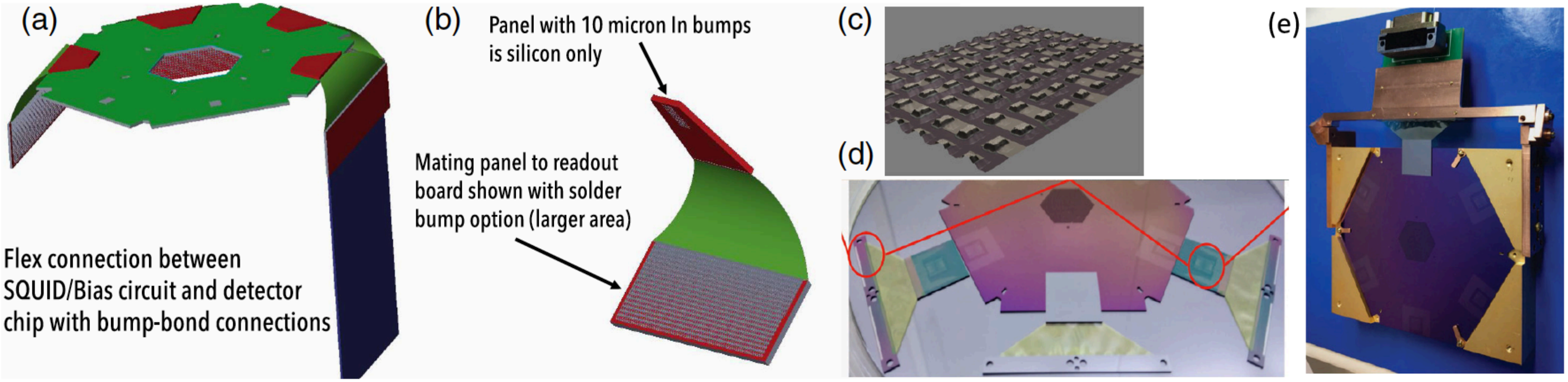

Fig. 17 (a) Illustration showing how bump-bonded connections are made between the detector chip and the side panels containing the readout. (b) Illustration showing the geometry of the flex and bumps. (c) Scanning electron microscope image of some prototype indium bumps fabricated and bump-bonded at GSFC. (d) Photograph a hexagonal detector chip connected to several silicon chips with wire-bond pads using superconducting microstrip flex and bump-bond connections. (e) Set-up for testing the bump-bonded connections between two chips through flex with superconducting microstrip.